ISSN 1330-3651 (Print), ISSN 1848-6339 (Online)
Received: 12 June 2025; Accepted: 25 August 2025

https://doi.org/10.17559/TV-20250612002740
Original scientific paper

High-Efficiency MPPT Strategies for Floating and Conventional Solar PV: A Simulation-Based Study

Saad CHAYMA, Aymen FLAH, Habib KRAIEM*, Ahmad A. MOUSA, Claude Ziad EL-BAYEH

Abstract: Solar photovoltaic (SPV) systems are an environmentally friendly and recyclable source of renewable energy. Direct connection of solar panels to the load results in suboptimal power provision. Therefore, getting the maximum performance from the SPV system is essential to improve efficiency. Various techniques have been proposed to track the maximum power point (MPPT) of the SPV system. Traditional MPPT techniques are usually limited to uniform weather conditions. This paper presents a comprehensive comparative analysis of Maximum Power Point Tracking (MPPT) techniques employed in conventional and floating solar photovoltaic (PV) systems. The study examines various MPPT techniques, including perturb and observe (P&O), particle swarm optimization (PSO), and artificial neural networks (ANN), in both conventional and floating solar photovoltaic systems. The simulations were performed in a MATLAB/Simulink environment. The results of the comparison of MPPT algorithms in this study show that all these algorithms display very high-efficiency rates, generally above 97%, indicating good overall performance of MPPT systems. Still, the ANN and PSO techniques remain at the top. It is also worth noting that FPV systems tend to produce more power than LPV systems, particularly in the summer.

Keywords: artificial neural network; floating photovoltaic system; incremental conductance; land-based system; MPPT techniques; particle swarm optimization; perturb and observe

1 INTRODUCTION

Photovoltaic (PV) systems are considered more efficient than other renewable energy sources due to their environmental and economic advantages. PVs represent the most promising renewable energy source because they are clean, inexhaustible, low-polluting, and require little maintenance. The main advantages of PV systems are that they contain no moving parts and do not generate noise. PV systems convert solar energy obtained from the sun into electrical energy. PV systems have lower efficiency compared to other renewable energy sources.

Solar energy is a plentiful and universally available resource, and photovoltaic (PV) systems represent one of the most widely adopted technologies to exploit it. PV modules are recognized for their efficiency, sustainability, and minimal environmental impact [1]. Nonetheless, traditional solar installations demand considerable land surface, which is an increasingly valuable asset. Leveraging large bodies of water for PV deployment can mitigate both land usage and operational expenses associated with energy production. As a result, floating solar PV (FPV) systems emerge as a viable and cost-effective alternative for maximizing solar energy utilization while improving the overall economic viability of solar projects. Research indicates that floating PV systems not only help address land scarcity but also achieve an average efficiency that is 11% greater than that of land-based PV (LPV) system [2]

Floating solar systems take advantage of the natural cooling effect of water, which improves their energy conversion efficiency and leads to higher electricity output compared to ground-mounted or rooftop PV installations [3]. These systems generally exhibit superior performance compared to conventional land-based PVsystems. The efficiency of a photovoltaic system, including the impact of various losses, is often measured using the performance ratio (PR). Because water cools, lowering temperature-related efficiency losses, FPV has the highest PR, usually between 0.75 % and 0.85% [4]. In contrast, the inland photovoltaic systems generally show lower PR values, ranging from 0.65 % to 0.78 %, due to greater exposure to dust accumulation and elevated operating temperatures. Systems typically achieve the highest specific energy yield, while the other systems tend to have the lowest yield. Floating PV systems experience the lowest temperature-related energy losses due to the natural cooling effect of water [5]. In comparison, LPV systems are more susceptible to temperature losses, as they are fully exposed to direct sunlight and lack any form of passive cooling. A similar pattern is observed with soiling losses: LPV installations are more prone to dust and dirt accumulation, whereas FPV systems benefit from reduced particulate buildup due to their waterborne placement [6]. However, because FPV setups require floating electrical components and are often situated further from the shore, they tend to incur slightly higher transmission losses compared to LPV systems, which benefit from direct land-based connections (Tab. 1).

Table 1 Comparative performance analysis of FPV and LPV systems

Parameters	FPV	LPV
Performance ratio (PR %)	0,75-0,85	0,65-0,78
Specific yield	High	Low
Temperature losses	Low	High
Soiling losses	Low	High
Shading losses	Low	Low
Transmission losses	Medium	Low

Solar energy primarily depends on temperature and solar radiation conditions [7]. With slight changes in solar radiation and temperature values, the maximum possible power generation of a solar PV system will also change. To enhance power output and improve the system's photovoltaic (PV) efficiency, maximum power point tracking is crucial [8]. Typically, a boost converter is linked between the load and the PV sources to facilitate the connection of an MPPT controller, which tracks the maximum power point (MPP). Many algorithms have been developed, but traditional methods such as perturb and observe (P&O) and incremental conductance (INC) are widely used due to their simplicity. However, these methods suffer from high energy losses. The development of computing power and microcontrollers has led to the emergence of techniques such as fuzzy logic controller (FLC) [9], particle swarm optimization (PSO) artificial

neural network (ANN) [10], Adaptive Neuro-Fuzzy Inference System (ANFIS) , hybrid models and others.

However, choosing an MPPT for a particular PV system design and situation can be confusing, as each approach has advantages and disadvantages. This paper aims to conduct a comparative study to identify the most effective MPPT methods, including perturb and observe (P&O), Incremental Conductance (InC), particle swarm optimization (PSO), and artificial neural networks (ANN), for both floating and conventional PV systems [11]. The MATLAB/SIMULINK platform used to model and obtain results shows that the ANN technique provided significant advantages over other proposed techniques.

2 FLOATING PHOTOVOLTAIC SYSTEM (FPVs)

Floating photovoltaic (FPV) systems are an innovative approach to generate renewable energy by installing solar panels on bodies of water, including lakes, reservoirs, ponds, and even oceans. Unlike traditional land-based solar farms, FPV systems are installed on floating structures that are fixed to the bottom of a water body or the coast. These floating platforms are designed to support the weight of solar panels and other related equipment, provide stability, and withstand various weather conditions, including wind and waves. Solar panels use the photovoltaic effect to convert sunlight into electricity, similar to land-based systems. The electricity generated is transmitted via submarine cables to land facilities, which can be incorporated into the grid or used to power nearby areas [12].

A typical FPV system comprises several key components, each serving a specific function to ensure efficient energy generation and system stability, as shown in Fig. 1.

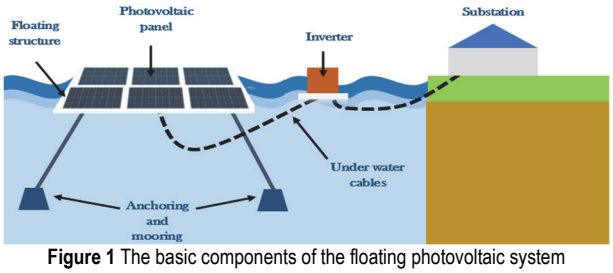

Figure 1 The basic components of the floating photovoltaic system

Floating platforms are the foundational element of floating photovoltaic (FPV) systems, providing the necessary buoyancy and stability for solar panels. These platforms are typically constructed from durable materials such as high-density polyethylene (HDPE), which are designed to withstand the challenging conditions of aquatic environments. The solar panels used in FPV systems are similar to those found in land-based installations and are securely mounted on these floating structures. To ensure the stability of the floating platforms, anchoring and mooring systems are essential. These systems prevent the platforms from drifting due to wind or water currents. They are usually customized to suit specific site conditions, considering factors like water depth, wave action, and soil type.

Additionally, underwater cables play a critical role in transmitting the electricity generated by the solar panels to onshore facilities. These cables are engineered to resist water ingress and mechanical damage, ensuring reliable electricity transfer. Inverters are another vital component of FPV systems, responsible for converting the direct current (DC) produced by the solar panels into alternating current (AC), which is compatible with the electrical grid or can be used by end-users. Finally, monitoring and control systems are implemented to oversee the operation of the FPV installation [2]. These systems ensure optimal performance by providing real-time data on energy production, weather conditions, and overall system status, allowing for efficient management and maintenance of the FPV system.

Floating photovoltaic systems (FPV) offer numerous advantages for renewable energy production. They allow for the exploitation of solar energy while preserving agricultural or urbanizable land, which is particularly useful in densely populated areas. Installed on water, FPVs benefit from a natural cooling effect, improving the efficiency of solar panels and reducing the risk of overheating. Moreover, they reduce water evaporation, limit algae proliferation, and can be integrated into hydroelectric dams for combined and stable energy production. Their reduced exposure to dust decreases maintenance needs. However, FPVs also have disadvantages. Their installation requires specific floating structures, costly anchoring and fastening systems. Maintenance on the water is more complex, and components can suffer degradation due to corrosion, biofouling, and climatic conditions [13]. These systems can also disrupt aquatic ecosystems and pose increased electrical risks due to the constant proximity to water. Thus, despite their high potential, rigorous design and maintenance are essential to ensure their sustainability and safety.

3 MODELLING OF THE OVERALL SYSTEM

3.1 PV Panels

The output current (I) of the PV cell is given by Eq. (1) [14]:

$$I = I_{\text{ph}} - I_0 \cdot \left(\exp\left(\left(\frac{q \times (V + I \cdot R_{\text{s}})}{n \cdot K \cdot T} \right) \right) - 1 \right) - \frac{V + I \cdot R_{\text{s}}}{R_{\text{sh}}} \quad (1)$$

where: I is the solar cell current; I_0, I_{S} is the saturation current of the diode (A); V is the output voltage of the PV cell (V); R_{s} is the series resistance (Ω); R_{sh} is the shunt resistance (Ω); n represents the ideality factor of the diode; q is the charge of electron (1.60217×10^{-19} C) and K is the Boltzmann constant (1.3807×10^{-23} J/k).

The photocurrent (I_{ph}) is proportional to the solar irradiance and varies with temperature. It is represented in Eq. (2):

$$I_{\text{ph}} = \left(I_{\text{sc,ref}} + \alpha_i \cdot (T - T_{\text{ref}}) \right) \cdot \frac{G}{G_{\text{ref}}} \quad (2)$$

where: $I_{\text{sc,ref}}$ is the short-circuit current at reference conditions; α_i is the temperature coefficient of short-circuit current and G_{ref} and T_{ref} are representative of the reference irradiance and temperature, respectively.

The reverse saturation current (I_0) is temperature dependent and defined as Eq. (3):

$$I_0 = I_{0,\text{ref}} \cdot \left(\frac{T}{T_{\text{ref}}}\right)^3 \cdot \exp\left(\frac{q \cdot E_g}{n \cdot k} \cdot \left(\frac{1}{T_{\text{ref}}} - \frac{1}{T}\right)\right) \quad (3)$$

where: E_g is the bandgap energy of the semiconductor.

Photovolatic modules are the fundamental building blocks of solar power systems. Each module consists of multiple PV cells elecrically interconnected to achieve the desired voltage and current ratings. The output current of the PV module is governed by Eq. (4) [15]:

$$I = I_{\text{ph}} \cdot N_p - I_0 \cdot N_p \cdot \left(\exp\left(\frac{\left(V + I \cdot R_s \cdot \frac{N_s}{N_p}\right)}{n \cdot k \cdot T \cdot N_s}\right) - 1\right) - \frac{V + I \cdot R_s \cdot \frac{N_s}{N_p}}{R_{\text{sh}} \cdot \frac{N_s}{N_p}} \quad (4)$$

Fig. 2 and 3 show the properties of the PV module under various temperatures and solar radiation levels.

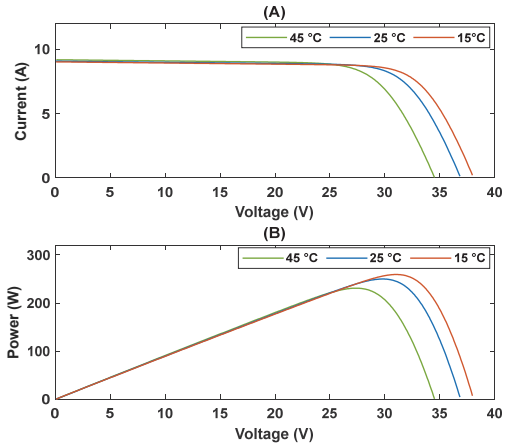

Figure 2 a) I-V curves at 25 °C for different irradiation levels; b) P-V curves under the same conditions

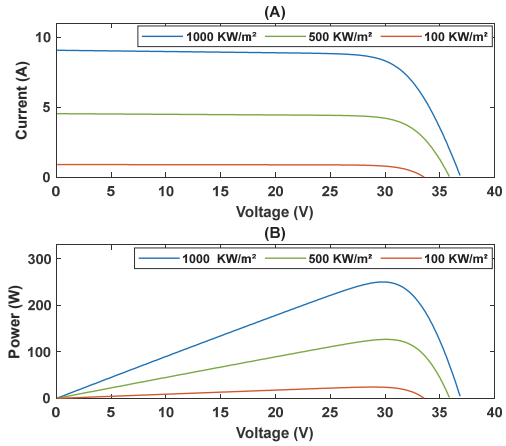

Figure 3 a) I-V curves at 25 °C for different irradiation levels; b) P-V curves under the same conditions.

3.2 Boost Converter

The boost converter is a switch-mode regulator that converts an unregulated DC voltage into a regulated DC output. Fig. 4 illustrates the components of a boost converter, which include a switch (such as a transistor or MOSFET), a diode, a filter capacitor, an inductor, and a resistor.

In a boost converter, the input voltage (V_i) and output voltage (V_o) are mathematically related as follows Eq. (5):

$$\frac{V_o}{V_i} = \frac{1}{1-d} \quad (5)$$

where: d is the duty cycle of the boost converter.

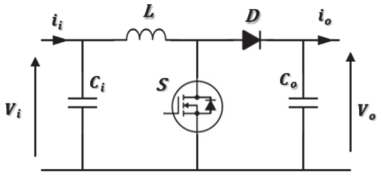

Figure 4 Schematic representation of the DC-DC boost converter

4 MAXIMUM POWER POINT TRACKING (MPPT): DIFFERENT TOOLS

4.1 Perturb and Observe (P&O) Algorithm

Due to its simplicity and ease of implementation, the Perturb and Observe (P&O) technique is the most commonly used method (Jain et al., 2018). The maximum power point is obtained when $\frac{dP}{dV} = 0$ $\frac{dP}{dV} = 0$.

The basic working principle of the P&O method is that when ΔP is positive and ΔV is positive, the increase continues in the direction of the MPP. If ΔP is positive and ΔV is negative, the MPP continues to increase, but in the opposite direction. If ΔP is negative and ΔV is positive, the MPP continues to grow from the opposite direction. If ΔP is negative and ΔV is negative, the increase continues in the same direction as the MPP until the maximum power p is reached. Fig. 5 shows the flowchart of the P&O algorithm.

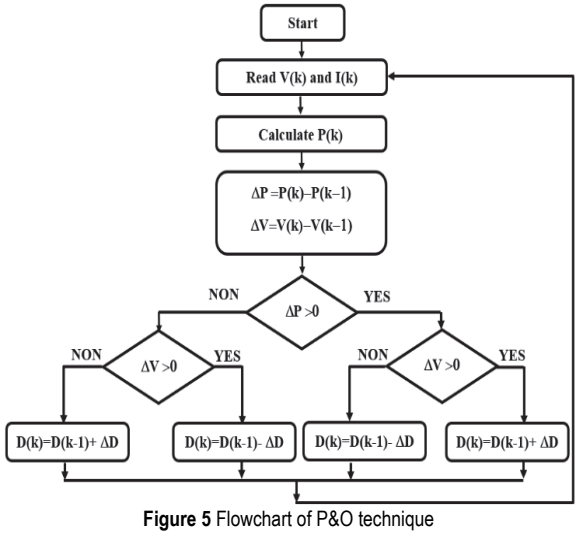

Figure 5 Flowchart of P&O technique

4.2 Incremental Conductance (InC) Algorithm

The incremental conductance (INC) algorithm was proposed to overcome some shortcomings of the P&O algorithm. The principle of the algorithm is to deduce the position of the operating point relative to the maximum power point based on the knowledge of the conductance and the conductance increment. The duty cycle is reduced if the conductance increment is greater than the opposite conductance. On the other hand, if the conductance increment is less than the opposite conductance, the duty cycle is increased. This process is repeated until the performance point is reached. Fig. 6 illustrates the flowchart of the P&O algorithm that describes the principle.

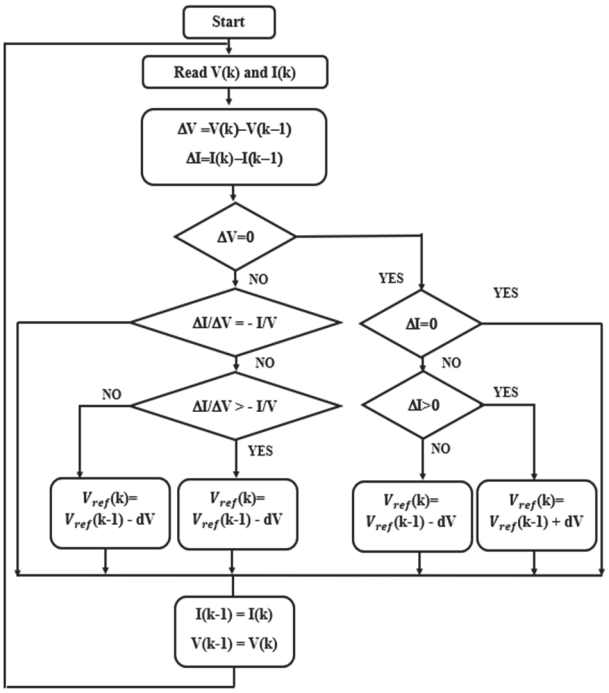

Figure 6 Flowchart of InC technique

4.3 Particle Swarm Optimization (PSO) Algorithm

The particle swarm optimisation (PSO) algorithm was developed by Kennedy and Eberhart in 1995 (Abdulla, 2021). The algorithm is based on a swarm that moves randomly in the search space. Each element in the swarm is referred to as a particle, and the speed and position of these particles are tracked. The particles move at a certain speed to reach the best position of the swarm. Based on the particle's best position and the swarm's best position, the value is updated in each iteration to reach the optimal solution [16].

The PSO algorithm randomly determines the initial position of the first particle, then guides its subsequent particles to search for the optimal value by updating their positions. In each iteration, each particle updates its position based on the best solution of the best local value (p_{best}) and the best solution based on the global population (g_{best}). Then, the velocity and position of the particle are updated using Eqs. (6) and (7). The parameters of the PSO algorithm are shown in Tab. 2. In addition, the flowchart of the PSO algorithm is shown in Fig. 7.

$$v_i(t+1) = w \cdot v_i(t) + c_1 \cdot rand_1 \cdot \left(p_{\text{best},i} - x_i(t)\right) + \\ + c_2 \cdot rand_2 \cdot \left(g_{\text{best}} - x_i(t)\right) \tag{6}$$

$$x_i(t+1) = x_i(t) + v_i(t+1) \tag{7}$$

where $v_i(t)$ is the velocity of i^{th} particle, $x_i(t)$ is the position of i^{th} particle, t is the current iteration, w is the inertia weight, $rand_1$ and $rand_2$ are the random (between 0 and 1), c_1 and c_2 are the cognitive and social coefficients, respectively, $p_{\text{best},\,i}$ is the best position of each particle and g_{best} is the best position among all particles.

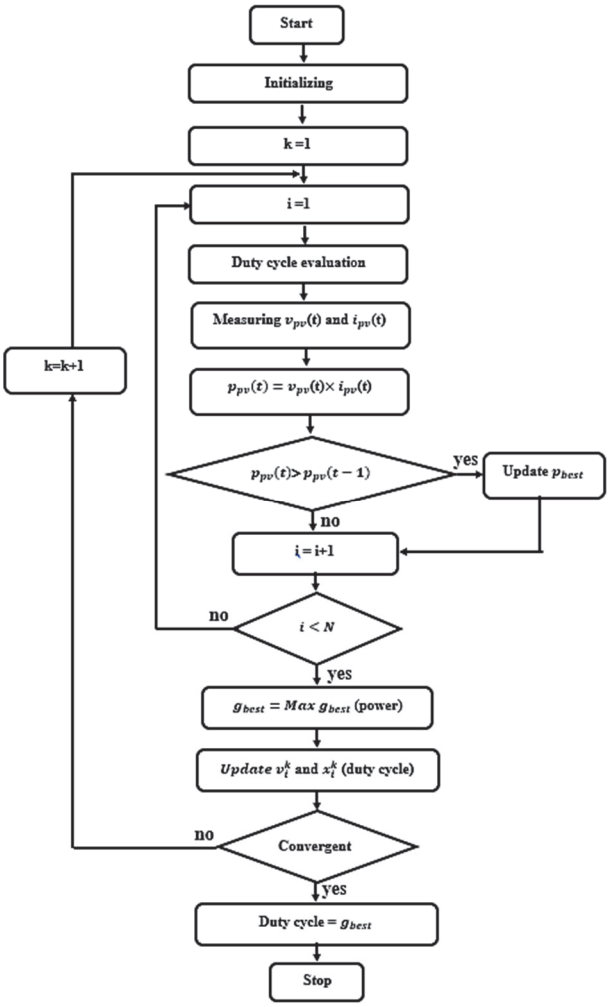

Figure 7 Flowchart of PSO technique

4.4 Artificial Neural Network (ANN) Algorithm

Artificial Neural Networks (ANN) are one of the most commonly used machine learning techniques in various applications. Compared to traditional methods, this technique offers several advantages. It is a computational model that requires training data to provide estimated outputs. In this paper, an artificial neural network (ANN) is employed to calculate the maximum voltage of a photovoltaic module, utilising solar irradiance and temperature as inputs. The training data is based on real measured and recorded signals [17].

The steps involved in creating an ANN are as follows:

- Collecting data;
- Selecting the ANN structure;
- Training the ANN;
- Testing the ANN.

Fig. 8 presents the overview of ANN in MPPT, where the inputs are solar temperature and irradiance. The neural network is targeting output is the DC-DC converter's duty ratio. For every solar temperature and irradiance fluctuation, the network outputs a specific duty ratio to reach the maximum power point.

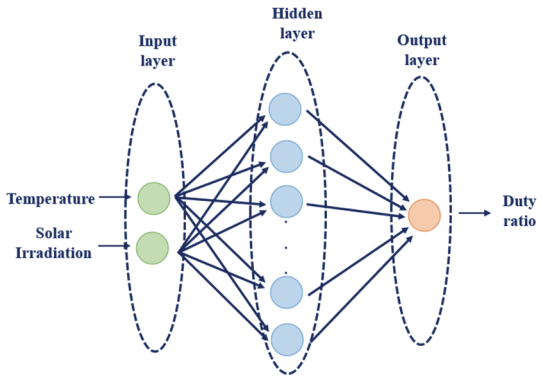

Figure 8 Structure of the used ANN

The Simulink model consists of an input layer with two neurons, a hidden layer with ten neurons, and an output layer with one neuron. The model is analysed using the Levenberg-Marquardt method. Fig. 9 shows the neural network model.

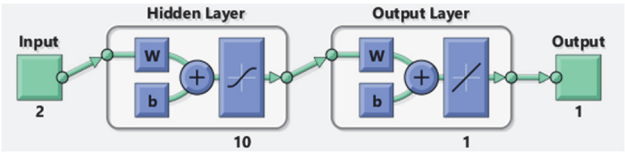

Figure 9 Layout of Trained ANN model

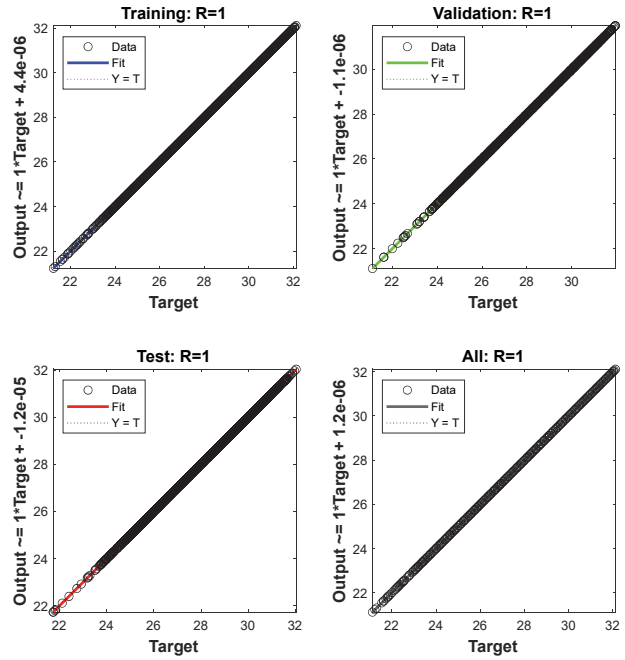

Figure 10 Regression plot of the ANN model

The Levenberg-Marquardt back-propagation algorithm is used to train neural networks. Fig. 10 shows the regression curve of the ANN-MPPT model training performed in this work. It can be seen that the coefficient (R) equals 1 ($R = 1$), indicating that our ANN-MPPT model training was 100% successful.

5 RESULTS AND DISCUSSION

Following the modelling of the photovoltaic (PV) system, MATLAB/Simulink software was utilized to perform a detailed comparison of the Perturb and Observe (P&O), Incremental conductance (InC), Particle Swarm Optimization (PSO), and Artificial Neural Network (ANN) maximum power point tracking (MPPT) technologies. These comparisons were conducted for both floating photovoltaic (FPV) and land-based photovoltaic (LPV) systems to evaluate the effectiveness and adaptability of the MPPT techniques under diverse environmental conditions.

In this analysis, real-world data were collected for average solar irradiation, temperature and wind speed (Fig. 11, Fig. 12, and Fig. 13) values at a selected site, ensuring a realistic representation of the environmental variables affecting the PV systems. This data set encompasses the four distinct seasons winter (December, January and February), spring (March, April and May), summer (June, July and August) and autumn (September, October and November) providing a comprehensive view of the system's performance throughout the year.

The FPV and LPV systems were tested under identical environmental inputs to allow a fair comparison of the MPPT techniques. Seasonal variations, such as the lower solar intensity in winter and the higher temperatures in summer, were particularly considered to understand the impacts on energy extraction and system efficiency. These seasonal effects and the performance differences between the two PV setups are illustrated in Fig. 12 and Fig. 13, which show the comparison of power outputs and tracking efficiency for the MPPT methods.

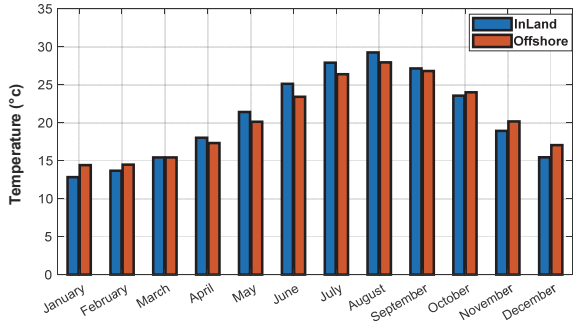

Figure 11 Temperature profile in both inland and at sea places

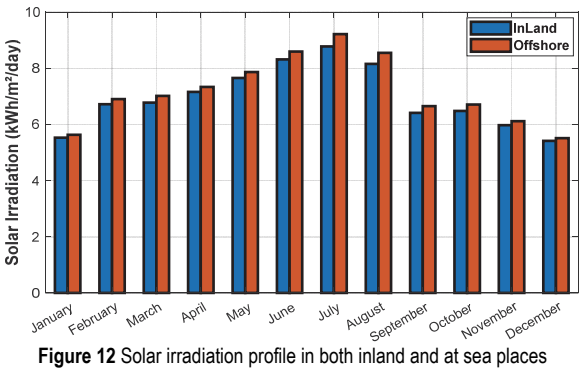

Figure 12 Solar irradiation profile in both inland and at sea places

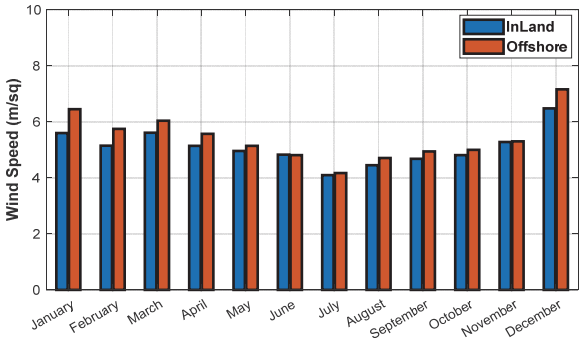

Figure 13 Wind speed profile in both inland and offshore places

By leveraging these results, the study provides insights into the suitability of P&O, InC, PSO, and ANN technologies for floating and conventional PV applications, emphasising their potential advantages and limitations under varying climatic conditions.

According to Fig. 11, overall, inland temperatures are consistently higher than offshore temperatures, particularly during the summer months (May to September), where the difference can reach 2 to 3 °C. Fig. 13 clearly illustrates the influence of geographical location on annual solar irradiation, with an offshore site consistently favoured over an inland site, possibly due to more favourable atmospheric conditions or the proximity to water, and depending on Fig. 14, the inland and offshore sites show a similar seasonal variation: stronger in winter, weaker in summer. For the offshore place, the sea winds are often more regular and stronger, the absence of obstacles (buildings, forests, terrain) allowing for a higher speed. About the inland place, the roughness of the terrain and obstacles reduce the average wind speed.

5.1 Results of the Simulation in Four Seasons in Both Systems: Floating and Inland

Fig. 14 illustrates the power production in the land-based PV system during 4 seasons with the four types of MPPT algorithms. Fig. 15 depicts the power generation of the floating PV system during the four seasons using various MPPT algorithms.

Table 2 Power results comparison among P&O, INC, PSO and ANN MPPT techniques

	P&O		PSO		ANN		INC	
	FPV	CPV	FPV	CPV	FPV	CPV	FPV	CPV
Winter	2430	2376	2542	2492	2561	2514	2430	2389
Spring	2957	2919	3085	3068	3099	3051	2957	2934
Summer	3564	3404	3622	3431	3581	3176	3564	3411
Autumn	2617	2534	22672	2591	2649	2466	2617	2542

Table 3 Efficiency (%) results comparison among P&O, PSO and ANN MPPT techniques

	P&O		PSO		ANN		INC	
	FPV	CPV	FPV	CPV	FPV	CPV	FPV	CPV
Winter	97,4	97,34	97,36	97,3	97,43	97,37	97,4	97,09
Spring	97,86	97,59	97,83	97,82	97,87	97,83	97,86	97,61
Summer	97,22	97,14	98,16	98,05	98,16	97,96	98,02	97,89
Autumn	97,28	97,5	97,49	97,41	97,5	97,38	97,38	97,27
Average	97,44	97,39	97,71	97,64	97,74	97,63	97,66	97,46

In each case, all the algorithms quickly reach the maximum power point, generally in less than 0.1 seconds, but with notable differences in terms of stability and efficiency. The ANN (in blue) and PSO (in green) algorithms consistently achieve a higher and more stable final power, reflecting better accuracy in tracking the maximum power point. Conversely, the P&O algorithm (in yellow) proves to be the least effective, with more pronounced oscillations and lower power. The INC algorithm (in red) shows intermediate results.

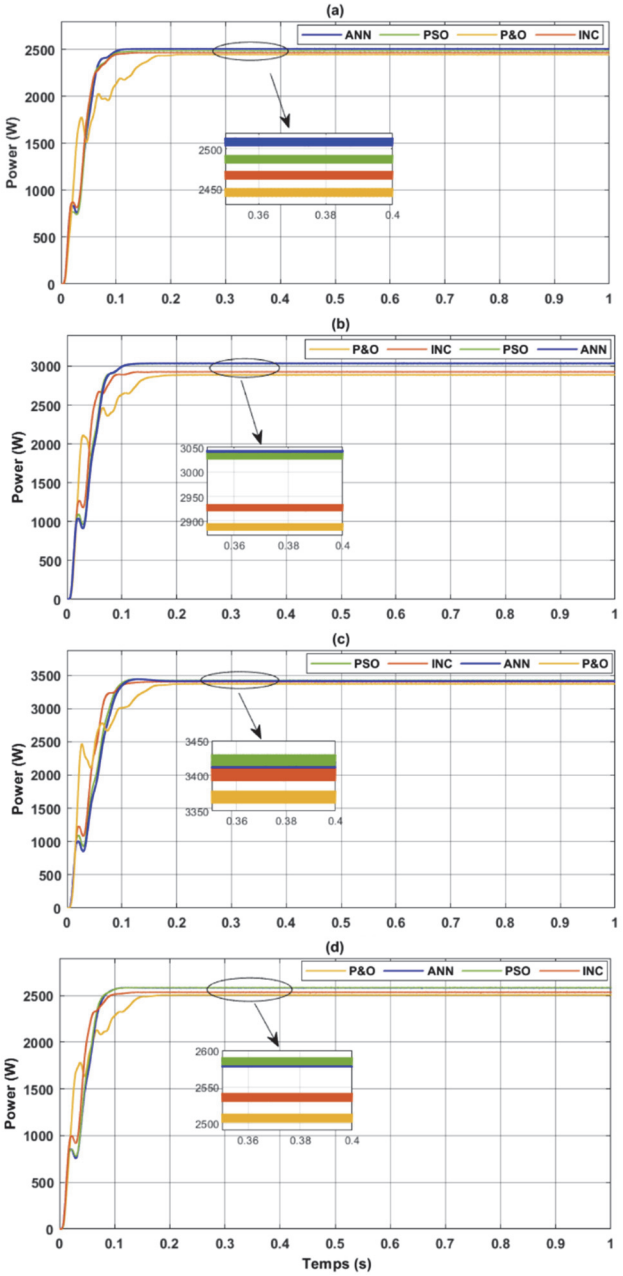

Figure 14 Power production for the three techniques in the LPV system for: (a) winter; (b) spring; (c) summer and (d) autumn

Based on convergence speed, stability, maximum extracted power, and average efficiency and power metrics, the ANN (artificial neural network) algorithm appears to be the best overall algorithm for both FPV and LPV systems. It offers superior or comparable performance to other algorithms in most seasonal conditions, characterized by rapid convergence, excellent stability, and very efficient maximum power extraction. The PSO algorithm is a very close competitor, often performing similarly to the ANN, but the ANN seems to have a slight overall advantage. P&O and INC, although functional, show limitations in terms of stability and

convergence speed compared to algorithms based on artificial intelligence (ANN, PSO).

It is also worth noting that the FPV system exhibits a higher overall performance gain than the LPV system across all seasons, due to its lower temperature profile, smaller shading area, and better cooling capacity compared to the other systems.

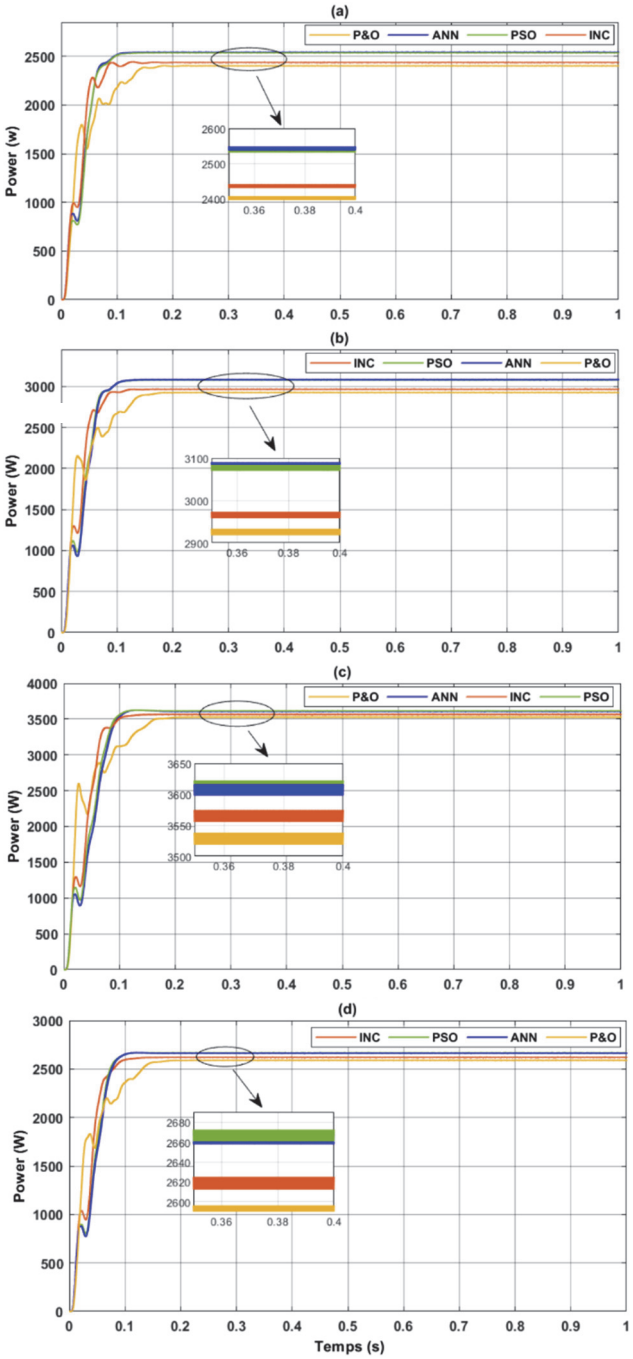

Figure 15 Power production for the three techniques in the FPV system for: (a) winter; (b) spring; (c) summer and (d) autumn

5.2 The Temperature Effect

Fig. 16 represents the temperature in the four seasons in the floating and the inland systems. It compares the average seasonal temperatures between two types of locations: seaside and inland. We observe the temperature variations for each season: winter, spring, summer, and autumn. In winter, the temperatures are the lowest, around 15 °C seaside and 14 °C inland, indicating a slight difference favoring the coastal areas. In spring, temperatures rise slightly, with 17 °C for the coast and 18 °C inland, showing a slight thermal superiority of the inland areas this time. In summer, the difference becomes more pronounced: inland areas reach around 28 °C compared to 26 °C for seaside areas, confirming a warmer trend inland. In autumn, temperatures drop again, with 24 °C offshore compared to 23 °C inland, where coastal areas become slightly warmer again. Generally speaking, inland areas experience greater temperature fluctuations according to the seasons, with hotter summers, while offshore areas enjoy a more moderate and stable climate.

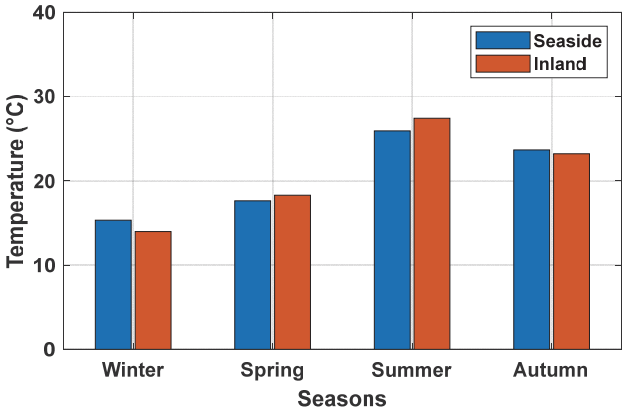

Figure 16 Temperature profile in both inland and sea places for four seasons

Temperature is a crucial factor that affects the maximum power of a PV module. High temperatures reduce efficiency and power.

From the previous figures (Figs. 14 and 15) representing the performance of MPPT algorithms under variable conditions, it is observed that temperature has a notable effect on the power produced by the floating PV system. An increase in temperature leads to a slight decrease in the maximum extracted power, which is consistent with the known behavior of photovoltaic cells. Despite this, the ANN and PSO algorithms show better stability in the face of thermal variations. They manage to maintain a more constant and higher power, even when the temperature varies. On the other hand, the P&O and INC algorithms are more sensitive, with a more pronounced drop in power and more oscillations. This underscores the importance of choosing a robust MPPT algorithm in environments subject to thermal fluctuations. Thus, PSO and ANN prove to be more suitable for optimal operation in real-world conditions.

6 CONCLUSIONS

Solar power systems are increasingly popular for generating clean electricity, but face challenges such as weather-related power fluctuations and shadowing. Therefore, tracking algorithms are essential for optimising energy production.

This paper compares three algorithms, namely P&O, InC, PSO, and ANN, for the floating and conventional solar PV systems. These techniques have been developed and tested in a MATLAB/Simulink environment; based on the simulation, it can be concluded that for both types of systems and all algorithms, the power produced varies

significantly depending on the seasons, with maximum power in summer and minimum power in winter. It is consistent with the variations in sunlight throughout the year.

FPV systems generally generate more power than CPV systems, especially during the summer, as mentioned in Tab. 2. This is likely due to the natural cooling effect of water used in FPV systems. The ANN and PSO algorithms typically show the best performance in most cases, with average efficiencies of 97.63% and 97.64% for the CPV system, and 97.74% and 97.71% for the FPV system, respectively, as it is summarized in Tab. 3. The INC algorithm outperforms the P&O algorithm, with a difference of 0.07% in the CPV system and 0.22% in the FPV system.

Acknowledgement

The authors extend their appreciation to Northern Border University, Saudi Arabia, for supporting this work through project number (NBU-CRP-2025-2484).

7 REFERENCES

[1] Zhang, B., Talihati, B., Fan, H., Sun, Y., & Wang, Y. (2025). A dynamic carbon flow traceability framework for integrated energy systems. *Journal of Cleaner Production*, *518*, 145878. https://doi.org/10.1016/j.jclepro.2025.145878

[2] Zhang, Y., Zhang, Y., Zheng, B., Cui, H., & Qi, H. (2025). Statistical analysis for estimating the optimized battery capacity for roof-top PV energy system. *Renewable Energy*, *242*, 122491. https://doi.org/10.1016/j.renene.2025.122491

[3] Qi, H., Zhou, Y., Zhang, Z., Wang, B., Zhang, Y., Cui, H., & Wang, X. (2020). Heat Transfer Performance in Energy Piles in Urban Areas: Case Studies for Lambeth College and Shell Centre UK. *Applied Sciences*, *10*(17), 5974. https://doi.org/10.3390/app10175974

[4] Li, Y., Li, H., Miao, R., Qi, H., & Zhang, Y. (2023). Energy-Environment–Economy (3E) Analysis of the Performance of Introducing Photovoltaic and Energy Storage Systems into Residential Buildings: A Case Study in Shenzhen, China. *Sustainability*, *15*(11), 9007. https://doi.org/10.3390/su15119007

[5] Zhu, L., Song, Y., Chen, H., Wang, M., Liu, Z., Wei, X., & Ai, T. (2025). Optimization of power generation and sewage treatment in stacked pulsating gas-liquid-solid circulating fluidized bed microbial fuel cell using response surface methodology. *International Journal of Hydrogen Energy*, *101*, 161-172. https://doi.org/10.1016/j.ijhydene.2024.12.397

[6] Ma, K., Yang, J., & Liu, P. (2020). Relaying-Assisted Communications for Demand Response in Smart Grid: Cost Modeling, Game Strategies, and Algorithms. *IEEE Journal on Selected Areas in Communications*, *38*(1), 48-60. https://doi.org/10.1109/JSAC.2019.2951972

[7] Zhong, Z., Burhan, M., Ng, K. C., Cui, X., & Chen, Q. (2024). Low-temperature desalination driven by waste heat of nuclear power plants: A thermo-economic analysis. *Desalination*, *576*, 117325. https://doi.org/10.1016/j.desal.2024.117325

[8] Zeng, Z. & Goetz, S. M. (2024). A General Modeling and Analysis of Impacts of Unbalanced Inductance on PWM Schemes for Two-Parallel Interleaved Power Converters. *IEEE Transactions on Power Electronics*, *39*(10), 12235-12248. https://doi.org/10.1109/TPEL.2024.3388024

[9] Zeng, Z. & Goetz, S. M. (2025). A Zero Common Mode Voltage PWM Scheme With Minimum Zero-Sequence Circulating Current for Two-Parallel Three-Phase Two-Level Converters. *IEEE Journal of Emerging and Selected Topics in Power Electronics*, *13*(2), 1503-1513. https://doi.org/10.1109/JESTPE.2024.3409290

[10] Yang, M., Jiang, Y., Guo, Y., Su, X., Li, Y., & Huang, T. (2025). Ultra-short-term prediction of photovoltaic cluster power based on spatiotemporal convergence effect and spatiotemporal dynamic graph attention network. *Renewable Energy*, *255*, 123843. https://doi.org/10.1016/j.renene.2025.123843

[11] Duan, X., Mi, W., Guo, S., Shen, C., & Kalogirou, S. A. (2025). Experimental investigation on a novel PV-Trombe wall for air heating and purification in the severe cold region. *Renewable Energy*, *248*, 123126. https://doi.org/10.1016/j.renene.2025.123126

[12] Shi, Z., Chen, J., Wang, Y., Zhao, Y., & Xu, B. (2025). Credibility Copula-Based Robust Multistage Plan for Industrial Parks Under Exogenous and Endogenous Uncertainties. *CSEE Journal of Power and Energy Systems*, *11*(3), 987-998.

[13] Niu, X., Ma, N., Bu, Z., Hong, W., & Li, H. (2022). Thermodynamic analysis of supercritical Brayton cycles using CO2-based binary mixtures for solar power tower system application. *Energy*, *254*, 124286. https://doi.org/10.1016/j.energy.2022.124286

[14] Wang, H., Wang, Y., Xiao, X., Ma, Z., & Xu, Q. (2025). Investigation on Transformer Inrush Current in Wind Farms Connected MMC-HVDC Systems. *Journal of Modern Power Systems and Clean Energy*, 1-11.

[15] Gao, S., Chen, Y., Song, Y., Yu, Z., & Wang, Y. (2024). An Efficient Half-Bridge MMC Model for EMTP-Type Simulation Based on Hybrid Numerical Integration. *IEEE Transactions on Power Systems*, *39*(1), 1162-1177. https://doi.org/10.1109/TPWRS.2023.3262584

[16] Meng, Q., He, Y., Li, S., Hussain, S., Lu, J., You, G., & Guerrero, J. M. (2025). Adaptive two-step power prediction and improved perturbation method for accelerated MPPT with reduced oscillations in photovoltaic systems. *Energy Reports*, *13*, 5328-5338. https://doi.org/10.1016/j.egyr.2025.04.055

Contact information:

Saad CHAYMA
University of Gabes,
National Engineering School,
Avenue Omar Khattab Gabes 6029, Tunisia
E-mail: saad.chayma@yahoo.fr

Aymen FLAH
1) Processes, Energy, Environment, and Electrical Systems,
National Engineering School of Gabès, University of Gabès, Tunisia
2) Applied Science Research Center, Applied Science Private University,
Amman, 11931, Jordan
3) College of Engineering, University of Business and Technology,
Jeddah, 21448, Saudi Arabia
E-mail: aymen.flah@enig.u-gabes.tn

Habib KRAIEM
(Corresponding author)
Department of Electrical Engineering,
College of Engineering, Northern Border University,
Arar, Saudi Arabia
E-mail: alhabeeb.kareem@nbu.edu.sa

Ahmad A. MOUSA
Department of Basic Sciences, Middle East University,
Amman 11831, Jordan
E-mail: amousa@meu.edu.jo

Claude Ziad EL-BAYEH
Department of Electrical Engineering,
Bayeh Institute, Amchit, Lebanon